First-principles study of the interfacial structures of Au/MgO(001)

D. Chen, X. L. Ma,* and Y. M. Wang
Shenyang National Laboratory for Materials Science, Institute of Metal Research, Chinese Academy of Sciences, Shenyang 110016, China

(Received 22 March 2006; revised manuscript received 19 December 2006; published 8 March 2007)

By using a first-principles method, the theoretical analysis of six probable Au/Mg(001) interface models points out that two of them with oxygen or magnesium vacancies in the interface are most stable. It is found in this work that besides O or Mg vacancies having to exist in this interface, the stability of an interface depends deeply on the atomic configuration of interface. Such a configuration in which each Au atom in the upper Au layer of interface bonds with each O atom in the MgO under layer is theoretically considered to be most stable. Nevertheless, these results need to be confirmed by experiments.

DOI: 10.1103/PhysRevB.75.125409 PACS number(s): 73.20.−r, 68.35.Ct, 31.15.Ar, 31.15.Ew

I. INTRODUCTION

The interface characteristic of metal oxides is often the controlling factor limiting their practical applications in catalysis, adhesion, corrosion, and microelectronics. Thus, determining it and understanding its influence are of great importance. For instance, although gold is one of the noblest metals and has little activity for chemisorption,[1] it was found that nanosize particles of gold supported on various oxides exhibit an enhanced catalytic activity,[2–4] which would be of great significance in environmental and chemical technologies, for example, to be used as a sensor.[5] Such a question of common interest stimulates many researchers to theoretically explain the interfacial behavior of metal oxides.[6–15] Many theoretical and experimental attempts have been done on the deposition and growth of Au clusters on MgO,[9,16–19] and some focused on adatoms and dimmers[6–8] and the adsorption characteristics on a regular MgO(001) surface;[9–11] however, they only concerned the adhesion of the isolated adatoms and adsorbed dimmers on the surface of oxide. A minority of them, such as the papers of Goniakowski[12] and Herschend *et al.*,[13] concentrated on the interfacial characteristics of metal coverages. To our best knowledge, the electronic structures of Au/MgO interfaces, which are physically and technologically important, remain unclear. Therefore, a systematic study of the Au/MgO interfaces is still needed. This is just our goal in the present paper.

II. COMPUTATIONAL DETAILS

As we know, it is possible to use first-principles calculations to study interface electronic structures and to acquire the results that agreed with experiments if the interface models used are reasonable.[20] In the present study of Au/MgO interfaces, the plane-wave pseudopotential (PWPP) method in the CASTEP code[21] has been employed.

In the calculations, the energy cutoff was set at 350 eV (25.7 Ry), which is a better choice with respect to the computational efficiency and convergence,[22] and the number of k points within the irreducible wedge of the Brillouin zone was determined by the Monkhorst-Pack scheme.[23] A k-point mesh of $6\times6\times1$ was used to sample each computational cell. All the atoms in each computational cell were relaxed until its total energy difference between two steps is smaller than 1×10^{-5} eV/atom. The total energy was minimized by means of a conjugate gradient technique.[24] The ultrasoft pseudopotentials[25] of gold, magnesium, and oxygen were taken and optimized to determine the appropriate plane-wave basis set. The density-mixing scheme based on the Pulay algorithm[26] was used for self-consistent-field (SCF) calculation. The SCF tolerance was set at 1×10^{-6} eV/atom. The atomic calculations and the formation of the pseudopotentials were treated self-consistently through the local-density approximation (LDA). The LDA exchange-correlation functional has been used in this study, because recent studies about Au on oxides indicated that it can provide a better Au/MgO description.[27–30] By using the Gasteiger method,[31] the spatial distributions of electronic charge and electrostatic potential were calculated for a whole system or a selection of atoms. Partial density of states (PDOS) gives a qualitative treatment on the nature of electron hybridization in the system and can be produced for certain angular momenta on selected atoms. If more than one atom is selected, the contributions in each angular momentum channel from all selected atoms are added together.

Experimentally,[32] vacancies have been found on the surfaces of Au nanoparticles embedded in MgO. Even in MgO crystals, oxygen and magnesium vacancies still exist,[33] and recent experiments have directly observed these defects on the (001) surface of ultrahigh-vacuum cleaved single MgO crystals.[34] Thus, the interaction of Au with oxygen and magnesium vacancies must be taken into consideration in modeling and calculating of Au/MgO interface.

Practically, the most often observed defects in MgO are oxygen vacancies. They are in different charge states depending on the condition in which they are prepared. Once the vacancies are formed, their electronic structures could be changed by adding or removing electrons in them;[35] therefore, the oxygen and magnesium vacancies can be classified as positive, negative, and neutral by their charges. The neutral oxygen vacancies are generally stable in bulk MgO.[36] In what follows, we address ourselves firstly to calculating the formation energies of neutral oxygen and magnesium vacancies in bulk MgO and comparing them with the experimental and previous computational results to give a feasible evidence of our method.

TABLE I. Calculated lattice constant a, bulk modulus B_0, and band gap compared to experiments and other theoretical works of MgO.

	a (Å)	B_0 (GPa)	Band gap (eV)	Method	Reference
MgO	4.210	160	7.83	Expt.	37 and 38
	4.205	180		HF[a]	39
	4.248	153		FP KKR[b]	40
	4.160		5.20	LMTO[c]	41
	4.165	171	5.00	LDA	42
	4.212	149	4.65	LDA	This study

[a]Periodic Hartree-Fock theory.
[b]Full potential Korringa-Kohn-Rostoker Green's function.
[c]Linear muffin-tin orbital method.

We first employed the PWPP method to calculate lattice constant, bulk modulus, and band gap of MgO. Table I summarizes a comparison of experimental values and calculated results based on various methods. The good agreement is typical of that normally expected in LDA calculations.

Table II lists the calculated formation energy E_{form} for an O or a Mg vacancy generated in one unit cell and eight unit cells of MgO, respectively, and their comparison with the experiments and previous calculations. When one oxygen (magnesium) vacancy is formed in a $Mg_{m+1}O_{m+1}$ computational cell, which is $(m+1)/4$ MgO unit cells as large, the formation energy E_{form} can be expressed as follows:[36,43]

$$E_{\text{form}}^{\text{O}}(\text{for oxygen vacancy, } V) = E_{\text{tot}}(\text{Mg}_{m+1}\text{O}_m V) - [mE_{\text{MgO}} + E_{\text{Mg}}], \quad (1)$$

$$E_{\text{form}}^{\text{Mg}}(\text{for magnesium vacancy, } V') = E_{\text{tot}}(\text{Mg}_m V'\text{O}_{m+1}) + E_{\text{Mg}} - (m+1)E_{\text{MgO}}, \quad (2)$$

where $E_{\text{tot}}(\text{Mg}_{m+1}\text{O}_m\text{V})$ ($E_{\text{tot}}(\text{Mg}_m V'\text{O}_{m+1})$) is the total energy of the fully relaxed $\text{Mg}_{m+1}\text{O}_m\text{V}$ ($\text{Mg}_m V'\text{O}_{m+1}$) cell, $m+1$ is the number of either O or Mg atoms in the $\text{Mg}_{m+1}\text{O}_{m+1}$ computational cell without O (or Mg) vacancy, and E_{MgO} and E_{Mg} are the total energy of pure MgO and Mg crystals per MgO and per Mg, respectively. To avoid an estimate for the spin-polarization correction to the energy of the isolated oxygen atom, the formation energy of the magnesium vacancy is computed to be the energy required to completely remove a magnesium atom from the MgO. The formation energy value of Mg vacancy can be understood from a consideration of the electronic state position of the defect level in the fundamental gap of MgO.[43]

TABLE II. Comparison between the formation energies of vacancies calculated and measured experimentally in bulk MgO.

		Formation energy of vacancies (E_{form}, eV)	
Method	Reference	O vacancy (V)	Mg vacancy (V')
Expt.	33	1.53	
LDA[a]	36	0.40[b]	
DFT[c]	43	1.82	13.82
This study		1.23 (Mg_4O_3V)	8.69 ($\text{Mg}_3V'\text{O}_4$)
		1.24 ($\text{Mg}_{32}\text{O}_{31}V$)	8.89 ($\text{Mg}_{31}V'\text{O}_{32}$)

[a]LDA using mixed-basis pseudopotential techniques.
[b]In Ref 36, the formation energy is underestimated due to the absolute convergence error (0.5 eV) and the constraints of computational cell size.
[c]Stationary energy functional in density functional theory.

Table II shows that our results agree well with the experimental and other theoretical values, except for Ref. 36, for both one unit cell (Mg_4O_3V and $\text{Mg}_3V'\text{O}_4$) and eight unit cells ($\text{Mg}_{32}\text{O}_{31}V$ and $\text{Mg}_{31}V'\text{O}_{32}$) of MgO as larger computational cell, which demonstrates that the correct E_{form} can still be obtained in a smaller computational cell down to one unit cell of MgO. This provides a reasonable basis for constructing a model of Au/Mg(001) with appropriate size. It is also suggested that the use of the smaller computational cell is enough to calculate formation energy on a relaxation compromise between calculation accuracy and computational efficiency.

III. RESULTS AND DISCUSSION

A. Interface models and their interfacial energies

The experiments[44–47] have observed that Au can be deposited on a MgO(001) surface and often keeps a good epitaxial relation $(001)[100]_{\text{Au}} \| (001)[100]_{\text{MgO}}$ with the MgO substrate because the lattice mismatch is so small (3.1%) between Au(001) and MgO(001). Based on these, five possible three-dimensional computational cells of the Au/MgO(001) interface are given. Each one contains three Au(001) upper layers and three MgO(001) under layers, and periodic boundary condition is forced on it in the [100], [010], and [001] directions, respectively. In Fig. 1, only one Au(001) and one MgO(001) interfacial layer in these cells are schematically shown, from which it can be seen that the upper layer has two two-dimensional Au units and the under layer has four two-dimensional MgO units.

Figure 1(a) is the computational cell of perfect Au/MgO interface called model A, in which the central Au atom on Au(001) is just located on the top of the central O atom of

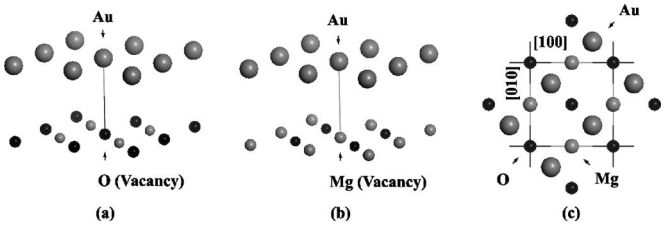

FIG. 1. Schematic diagrams of five computational cells of the Au/MgO(001) interface employed in present study. (a) is for models A and D, (b) for models B and E, (c) for model C (where the big gray spheres are Au, the small gray spheres are Mg, and the black spheres are O). The vacancy in model D or E is at the position of O or Mg atom removed.

MgO(001) along the [001] direction. It can be modified as model D, a computational cell of defective Au/MgO interface, if the central oxygen atom is removed. Model B (E) in Fig. 1(b) is the other computational cell of perfect (defective) Au/MgO interface; the only difference from Fig. 1(a) is that the central Au atom is on top of the central Mg atom (Mg vacancy). Figure 1(c) is a planform along the [001] direction of the computational cell of model C; this cell can be constructed by shifting the Au atoms $(\sqrt{3}/4)a_{\mathrm{MgO}}$ (a_{MgO} the lattice constant of MgO) along $[\bar{1}10]$ from model A shown in Fig. 1(a). For the defective models (D and E) in Figs. 1(a) and 1(b), the vacancy-vacancy distance between the neighbor computational cells is much larger than the corresponding typical value of vacancy radius, and the interaction between them could be negligible.

The interface energy E_{inter} ($\mathrm{J/m^2}$) of a perfect Au/MgO(001) interface computational cell of model A, B, or C in equilibrium state can be written as

$$E_{\mathrm{inter}} = \frac{1}{2S}\{E_{\mathrm{tot}}[\mathrm{Au/MgO}](n,N) - nE_{\mathrm{Au}} - NE_{\mathrm{MgO}}\}, \quad (3)$$

where $E_{\mathrm{tot}}[\mathrm{Au/MgO}](n,N)$ is the total energy of this cell in which n is the number of Au atoms in upper layers and N the number of Mg or O atoms in under layers, respectively; each cell has two interfaces; S is its interface area perpendicular to $[001]_{\mathrm{Au}}$ or $[001]_{\mathrm{MgO}}$; and E_{Au} and E_{MgO} are the total energies of Au and MgO crystal per Au and per MgO, respectively.

For the defective model D with O vacancy, the interface energy E_{inter} ($\mathrm{J/m^2}$) can be calculated by

$$E_{\mathrm{inter}} = \frac{1}{2S}\{E_{\mathrm{tot}}[\mathrm{Au/MgO}](n,N) - [nE_{\mathrm{Au}} + (N-2)E_{\mathrm{MgO}} + 2E_{\mathrm{Mg}} + E^{\mathrm{O}}_{\mathrm{form}}]\}, \quad (4)$$

where $E_{\mathrm{tot}}[\mathrm{Au/MgO}](n,N)$, S, E_{Au}, E_{MgO}, E_{Mg}, and $E^{\mathrm{O}}_{\mathrm{form}}$ have the same meaning as in Eqs. (1) and (3).

In model D, O vacancy at Au/MgO interface is embedded between MgO and Au layers. Thus, the vacancy formation energy should be $\frac{1}{2}E^{\mathrm{O}}_{\mathrm{form}} + \frac{1}{2}E^{\mathrm{Au}}_{\mathrm{form}}$, where $E^{\mathrm{Au}}_{\mathrm{form}}$ is the formation energy of vacancy in relaxed Au crystal. However, the calculated $E^{\mathrm{O}}_{\mathrm{form}} = 1.23$ eV and $E^{\mathrm{Au}}_{\mathrm{form}} = 0.21$ eV; the former is about 1 eV larger than the latter. Therefore, in Eq. (4), it is reasonable to use $E^{\mathrm{O}}_{\mathrm{form}}$ instead of the sum of the formation energies of oxygen vacancy in the two interfaces included in a computational cell.

For the defective model E with Mg vacancy, E_{inter} ($\mathrm{J/m^2}$) can be obtained by

$$E_{\mathrm{inter}} = \frac{1}{2S}\{E_{\mathrm{tot}}[\mathrm{Au/MgO}](n,N) + [E_{\mathrm{Mg}} + E^{\mathrm{Mg}}_{\mathrm{form}} + E^{\mathrm{Au}}_{\mathrm{repl}}] - [(n-1)E_{\mathrm{Au}} + NE_{\mathrm{MgO}}]\}, \quad (5)$$

where $E_{\mathrm{tot}}[\mathrm{Au/MgO}](n,N)$, S, E_{Au}, E_{MgO}, E_{Mg}, and $E^{\mathrm{Mg}}_{\mathrm{form}}$ have the same meaning as in Eqs. (2) and (3); $E^{\mathrm{Au}}_{\mathrm{repl}}$ is the energy when a Mg atom is replaced by a Au atom in MgO crystal. Similar to Eq. (4), the vacancy formation energy of magnesium at Au/MgO interface is calculated in the same way as in Eq. (4) for oxygen vacancy.

Table III lists the interface spacing and energy obtained from these fully relaxed models. Among all the perfect interface models A, B, and C, model A shown in Fig. 1(a) is the most stable since it has the smallest interface energy.

However, this case can be changed if vacancies appear in the Au/MgO interface. Model D is an obvious example. The presence of oxygen vacancy makes the interface energy of model D decrease to 0.535 $\mathrm{J/m^2}$ and makes the corresponding interfacial spacing between Au and O vacancy the smallest, 2.035 Å, among the five models. It seems that the interaction of Au with O vacancy is much stronger than with O atom itself, and thus, such interaction holds this interface to be more stable. From above elementary analysis, we can roughly predict that the cohesion of Au/MgO interface is closely relative to and determined by its interfacial structure.

At the end of this section, we should point out that the calculated results are less sensitive to the number of layers of

TABLE III. Interface spacing and energy calculated for models A, B, C, D, and E after they are fully relaxed.

Interface model	Interfacial status	Interface spacing (Å) (between Au and #)	Interface energy ($\mathrm{J/m^2}$)	Relaxation
A	Perfect	2.548 (#: O)	1.447	Yes
B	Perfect	3.007 (#: Mg)	2.018	Yes
C	Perfect	2.769 (#: interstitial site)	1.876	Yes
D	Defective	2.035 (#: O vacancy)	0.535	Yes
E	Defective	2.610 (#: Mg vacancy)	1.869	Yes

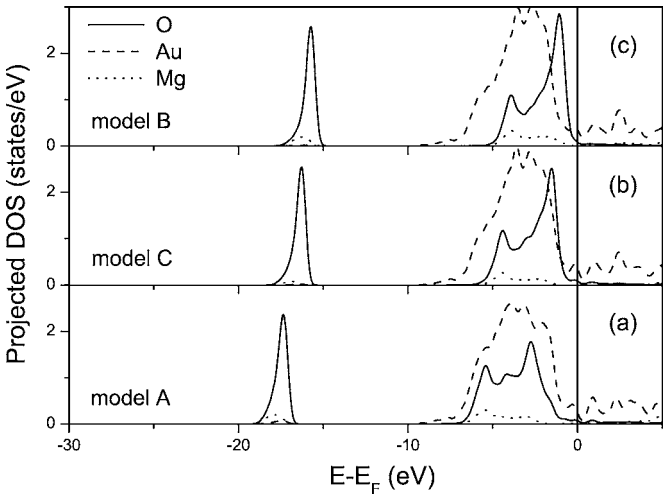

FIG. 2. Projected density of states of interfacial Au, O, and Mg for (a) model A, (b) model C, and (c) model B.

Au(001) and MgO(001) in a model if it is beyond a critical value. For instance, the calculated interface energies of model D are 0.521 and 0.513 J/m^2 for a five-Au(001)-layer–five-MgO(001)-layer and for a seven-Au(001)-layer–seven-MgO(001)-layer models, respectively, and only −0.014 and −0.022 J/m^2 less than 0.535 J/m^2 for the three-Au(001)-layer–three-MgO(001)-layer model. This indicated that the three-Au(001)-layer–three-MgO(001)-layer models we used are suitable for studying the electronic structures of Au/MgO(001) interfaces.

B. Perfect interface

Figure 2 shows the PDOSs of interfacial Au, O, and Mg in models A, C, and B, with respect to the Fermi level at zero. It can be found that the PDOSs of Au and O are predominant and much larger than that of Mg. The PDOS of Au is almost unchanged for three models but the PDOS of O shifts gradually to low-energy range from model B to C and then to A. As a result, the hybridization between 5*d*, 6*s* states of Au and 2*p* states of O in the energy range from 0 to −9 eV increases gradually from model B to C and then to A. This explains well the variations of interface spacing and energy E_{inter} for models A, B, and C listed in Table III.

Figures 3(a)–3(c) show the corresponding contour plots of the electron-density distribution for models A, B, and C. It can be clearly seen that the bonding across interface is stronger for model A, moderate for model C, and weaker for model B, which are consistent with the calculated results listed in Table III.

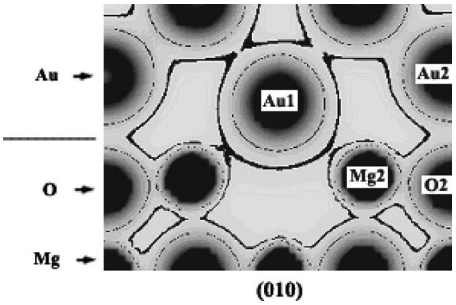

FIG. 4. Electron-density distribution in the (010) plane of model D. Two contour lines are labeled at 0.17 electrons/Å^3 (solid line) and 0.41 electrons/Å^3 (dashed line).

C. Defective interface

1. Oxygen vacancy interface

To explain why model D has so small E_{inter} from the view of electronic structure, we give its contour plots of the electron-density distribution in the (010) plane in Fig 4. Comparing it with Fig. 3(a) for model A, it can be found that due to the interface spacing going smaller from 2.548 to 2.035 Å, (1) the stronger metallic bonding forms between Au1 (just on the top of O vacancy) and the four neighbor Mg2 atoms by sharing electrons between Au 6*s* and Mg 3*s* orbitals, which can be demonstrated with charge increasing of Mg from 1.39 and Au from 0.2 in model A to 1.54 and 0.32 in model D; and (2) the covalent interactions are greatly strengthened between Au2 and O2 atoms in Fig. 4, because in this case, as shown in PDOS curves in Fig. 5(b), the hybridization between 5*d*, 6*s* states of Au2 and 2*p* states of O2 in the energy range from 0 to −9 eV is stronger than that in model A, as shown in Fig. 5(a).

From the above analysis, we can conclude that the appearance of O vacancy would be in favor of stability of Au/Mg(001) interface; thus, it may be probable to observe such an interface in experiments.

2. Magnesium vacancy interface

Figure 6(a) is the side view of the original model E along the [100] direction, in which Au atom is just on the top of the central Mg vacancy. Figure 6(b) is the contour plots of the electron-density distribution in the (010) plane for the fully

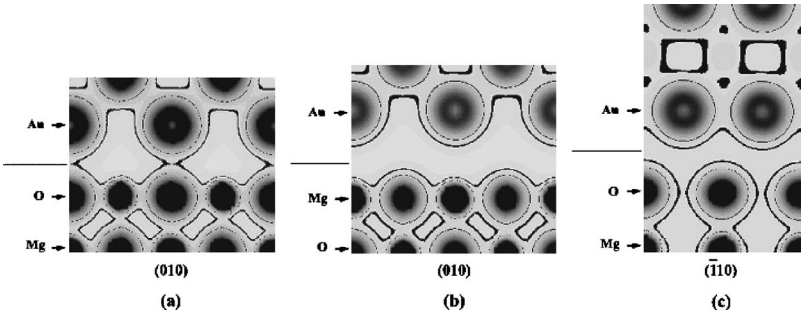

FIG. 3. Electron-density distribution for (a) model A at (010), (b) model B at (010), and (c) model C at ($\bar{1}$10). Two contour lines are labeled at 0.17 electrons/Å^3 (solid line) and 0.41 electrons/Å^3 (dashed line).

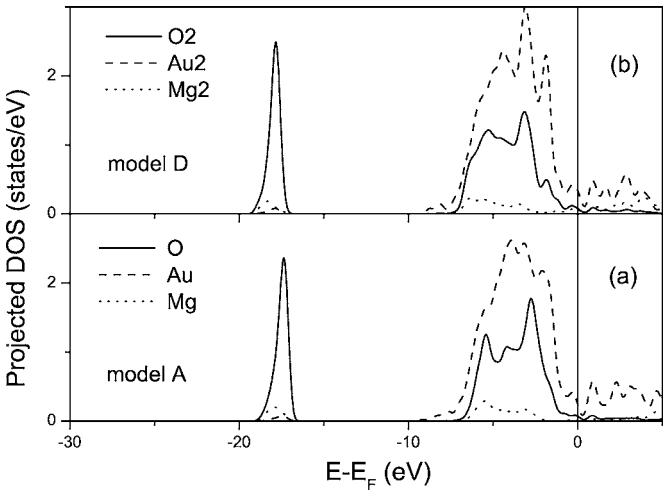

FIG. 5. (a) PDOSs of Au2, O2, and Mg2 shown in Fig. 4 for model D. (b) PDOSs of Au, O, and Mg in the Au/MgO interface for model A.

relaxed model E. In Fig. 6(b), it can be seen that Au atom moves down along the [001] direction and almost occupies the Mg vacancy, thus forming a vacancy in the upper Au layers.

For this model, $E_{\text{inter}}=1.869$ J/m^2 and interface spacing $=2.610$ Å. This interface is a bit stronger than that in model B, but must less stable than that in model D since it is kept mainly by weaker metallic bonds between Au and Mg.

This case will be changed if the upper three Au layers shown in Fig. 6(a) are shifted by $\frac{1}{2}a_{\text{MgO}}$ (a_{MgO} the lattice constant of MgO) along the [010] direction, called model F. Figure 7(a) shows the side view of model F along the [100] direction. Figure 7(b) gives its contour plots of the electron-density distribution on the (010) plane for fully relaxed model F. Due to the stronger covalent interactions between Au atoms in the upper layers and O atoms in the under layers, the interface energy E_{inter} of model F reduces to 0.468 J/m^2 and the interfacial spacing to 2.105 Å, which is comparable with model D. This means that model F may be also a probable Au/MgO interface observed. The common

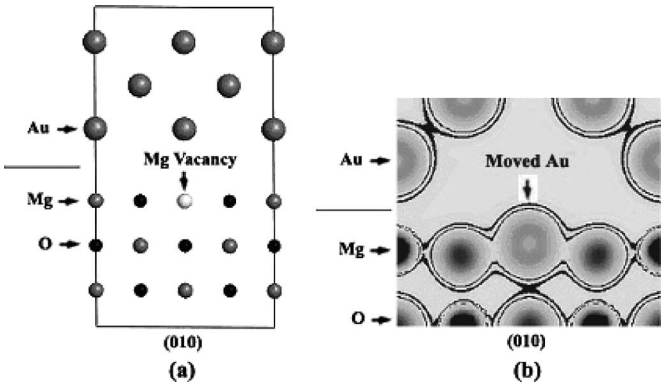

FIG. 6. (a) Side view of the original model E along the [100] direction. (b) Electron-density distribution in the (010) plane of model E, in which two contour lines are labeled at 0.31 electrons/Å^3 (solid line) and 0.51 electrons/Å^3 (dashed line).

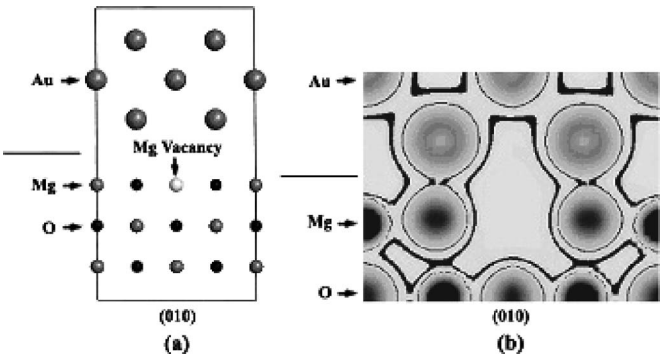

FIG. 7. (a) Side view of model F along the [100] direction. (b) Electron-density distribution in the (010) plane of model F, in which two contour lines are labeled at 0.21 electrons/Å^3 (solid line) and 0.56 electrons/Å^3 (dashed line).

characteristics of models D and F are that (1) vacancies appear in Au/MgO interfaces and (2) Au atoms in the upper layer of interface are just on the top of O atoms in the under layer.

D. Discussion

By performing an iterative process, geometry optimization allows us to refine the geometry of a structure to obtain a stable structure, in which the coordinates of the atoms and possibly the computational cell parameters are adjusted so that the total energy of the structure is minimized. For a consistent comparison, all of the six possible modes have been fully relaxed, not only in the vertical direction but also with lateral relaxation of atoms.

However, the important fact is found that the vertical and lateral movements of the interfacial atoms are very different after relaxations. The vertical movements of interfacial atoms are much larger in magnitude than lateral displacements of interface, because there is an interface stress determined by electrostatic interaction. Interface relaxation can strongly reduce the interface stress in the vertical direction, only leading to a relatively small lateral relaxation of interfacial atoms. This phenomenon is notable especially in the models with vacancies. For example, in model E in Fig. 6, geometry optimization showed that the Au atom just on the top of the Mg vacancy moves down along the [001] direction and almost occupies the Mg vacancy, but other interfacial atoms only slightly deviate from their original sites accompanied by the geometry relaxation.

For perfect Au/MgO(001) interfaces, our major result is that Au atoms prefer to be on the top of O atoms, agrees with results obtained by previous studies on the adhesion of Au atom on the MgO(001) substrate.[9,14,15] This was also observed in the experiments of Ag adsorption on MgO.[48,49] Especially, Giordano *et al.*[15] reported recently that the bonding between the Au and O atoms is twice as strong as the bonding between Au and Mg atoms on the adsorption of Au on MgO. All of these prove our models and calculations of Au/MgO(001) interfaces to be correct. Our study on model B indicates that the previous conclusion[50] that the over-

magnesium configuration is the most stable Au/MgO interface is inappropriate.

In our calculations, a small periodic computational cell is used. Therefore, the effect of mismatch between Au and MgO is underestimated than it does in practical Au/MgO interfaces; for example, in the practical "model D," Au atoms may be on the positions a bit far from the top of O atoms rather than exactly on the top of them.[51] The corresponding E_{inter} may not be exactly 0.535 J/m^2. However, we believe that the large difference of about 1–1.5 J/m^2 of models D and F from model A, B, C, and E may be not from the effect of mismatch but from the binding energy of the interfaces.

For the defective interface, three interface configurations (models D, E, and F) have been calculated to study the effect of vacancies on the Au/MgO(001) interface. Our calculations of models D and F demonstrated that both oxygen and magnesium vacancies are strong traps for metallic atom and make the interface spacing reduced; merely the effect of oxygen vacancy is stronger than magnesium vacancy. This is inconsistent with the general view that only O vacancies do so.[18,30,52–54] To reduce the Au/MgO interface energy, besides O or Mg vacancies reducing the interface spacing, the atomic configuration in an interface is a key. If Au atoms in the upper layer in the interface are arranged one to one on the top of O atoms in the MgO under layer, the strong covalent interactions between Au and O atoms will cohere tightly these two layers and form a stable interface as models D and F. In contrast to the Au to Mg atomic configurations as models B and E, the Au/MgO interfaces cohered mainly by Au–Mg metallic bonds are unstable.

IV. CONCLUSIONS

The first-principles plane-wave pseudopotential method is performed to study the electronic properties and bonding structures of the Au/MgO(001) interface. Six possible models A, B, C, D, E, and F of Au/MgO(001) interface are constructed, and the interface energies and interface spacings are calculated for them. We find that both oxygen and magnesium vacancies in a Au/MgO interface are strong traps for Au atoms and make the interface spacing reduced. The stability of a Au/MgO interface depends mainly on the atomic configuration in the interface. If (1) O and Mg vacancies exist in this interface, (2) the Au to O atomic configuration between the upper and under layers in the interface is formed; this interface is most stable as models D and F. We expect that such interfaces may exist in higher probability in Au/MgO interfaces, but they needed to be proven by experiments.

ACKNOWLEDGMENTS

This work was supported by the National Natural Science Foundation of China (Grants No. 50325101 and No. 10474102) and the Special Funds for the Major State Basic Research Projects of China (Grant No. 2002CB613503).

*Author to whom correspondence should be addressed. Electronic address: xlma@imr.ac.cn

[1] B. Hammer and J. K. Norskov, Nature (London) **376**, 238 (1995).
[2] G. V. Nazin, X. H. Qiu, and W. Ho, Science **302**, 77 (2003).
[3] A. Sanchez, S. Abbet, U. Heiz, W. D. Schneider, H. Häkkinen, R. N. Barnett, and U. Landman, J. Phys. Chem. **103**, 9573 (1999).
[4] H. Häkkinen, R. N. Barnett, and U. Landman, Phys. Rev. Lett. **82**, 3264 (1999).
[5] M. Haruta, Catal. Today **36**, 153 (1997).
[6] I. Moullet, Surf. Sci. **331-333**, 697 (1995).
[7] D. M. Duffy and J. A. Blackman, Phys. Rev. B **58**, 7443 (1998).
[8] G. M. Wang, J. J. BelBruno, S. D. Kenny, and R. Smith, Phys. Rev. B **69**, 195412 (2004).
[9] I. Yudanov, G. Pacchioni, K. Neyman, and N. Rösch, J. Phys. Chem. B **101**, 2786 (1997).
[10] A. Markovits, J. C. Paniagua, N. López, C. Minot, and F. Illas, Phys. Rev. B **67**, 115417 (2003).
[11] G. M. Wang, J. J. BelBruno, S. D. Kenny, and R. Smith, Surf. Sci. **576**, 107 (2005).
[12] J. Goniakowski, Phys. Rev. B **58**, 1189 (1998).
[13] B. Herschend, K. Hermansson, M. Alfredsson, Y. F. Zhukovsk III, E. A. Kotomin, and P. W. M. Jacobs, J. Phys. Chem. B **107**, 11893 (2003).
[14] G. Pacchioni, L. Giordano, and M. Baistrocchi, Phys. Rev. Lett. **94**, 226104 (2005).
[15] L. Giordano, M. Baistrocchi, and G. Pacchioni, Phys. Rev. B **72**, 115403 (2005).
[16] A. Sanchez, S. Abbet, U. Heiz, W. D. Schneider, H. Häkkinen, R. N. Barnett, and U. Landmann, J. Phys. Chem. A **103**, 9573 (1999).
[17] M. Kubo, R. Miura, R. Yamauchi, R. Vetrivel, and A. Miyamoto, Appl. Surf. Sci. **89**, 131 (1995).
[18] A. V. Matveev, K. M. Neyman, I. V. Yudanov, and N. Rösch, Surf. Sci. **426**, 123 (1999).
[19] K. Højrup-Hansen, S. Ferrero, and C. R. Henry, Appl. Surf. Sci. **226**, 167 (2004).
[20] D. Chen, X. L. Ma, Y. M. Wang, and L. Chen, Phys. Rev. B **69**, 155401 (2004).
[21] M. C. Payne, M. P. Teter, T. A. Arias, and J. D. Joannopoulos, Rev. Mod. Phys. **64**, 1045 (1992).
[22] J. S. Lin, A. Qteish, M. C. Payne, and V. Heine, Phys. Rev. B **47**, 4174 (1993).
[23] H. J. Monkhorst and J. D. Pack, Phys. Rev. B **13**, 5188 (1976).
[24] M. P. Teter, M. C. Payne, and D. C. Allan, Phys. Rev. B **40**, 12255 (1989).
[25] D. Vanderbilt, Phys. Rev. B **41**, 7892 (1990).
[26] P. Pulay, Mol. Phys. **17**, 197 (1969).
[27] Y. Shen and J. J. BelBruno, J. Chem. Phys. **118**, 9241 (2003).
[28] G. M. Wang, J. J. BelBruno, S. D. Kenny, and R. Smith, Surf. Sci. **576**, 107 (2005).
[29] Z. Yang, R. Wu, and D. W. Goodman, Phys. Rev. B **61**, 14066 (2000).
[30] Z. Yang, R. Wu, Q. Zhang, and D. W. Goodman, Phys. Rev. B **65**, 155407 (2002).

[31] J. Gasteiger and M. Marsili, Tetrahedron **36**, 3219 (1980).
[32] J. Xu, A. P. Mills, Jr., A. Ueda, D. O. Henderson, R. Suzuki, and S. Ishibashi, Phys. Rev. Lett. **83**, 4586 (1999).
[33] L. A. Kappers, R. L. Kroes, and E. B. Hensley, Phys. Rev. B **1**, 4151 (1970).
[34] C. Barth and C. R. Henry, Phys. Rev. Lett. **91**, 196102 (2003).
[35] A. M. Ferrari and G. Pacchioni, J. Phys. Chem. **99**, 17010 (1995).
[36] Q. S. Wang and N. A. W. Holzwarth, Phys. Rev. B **41**, 3211 (1990).
[37] O. L. Anderson and P. Andreatch, Jr., J. Am. Ceram. Soc. **49**, 404 (1966).
[38] R. C. Whited, C. J. Flaten, and W. C. Walker, Solid State Commun. **13**, 1903 (1973).
[39] M. I. McCarthy and N. M. Harrison, Phys. Rev. B **49**, 8574 (1994).
[40] A. N. Baranov, V. S. Stepanyuk, W. Hergert, A. A. Katsnelson, A. Settels, R. Zeller, and P. H. Dederichs, Phys. Rev. B **66**, 155117 (2002).
[41] U. Schönberger and F. Aryasetiawan, Phys. Rev. B **52**, 8788 (1995).
[42] H. Baltache, R. Khenata, M. Sahnoun, M. Driz, B. Abbar, and B. Bouhafs, Physica B **344**, 334 (2004).
[43] A. Gibson, R. Haydock, and J. P. LaFemina, Phys. Rev. B **50**, 2582 (1994).
[44] S. Giorgio, C. Chapon, C. R. Henry, G. Nihoul, and J. M. Penisson, Philos. Mag. A **64**, 87 (1991).
[45] T. Kizuka, T. Kachi, and N. Tanaka, Z. Phys. D: At., Mol. Clusters **26**, S58 (1993).
[46] T. Kizuka and N. Tanaka, Phys. Rev. B **56**, R10079 (1997).
[47] B. Pauwels, G. VanTendeloo, W. Bouwen, L. T. Kuhn, P. Lievens, H. Lei, and M. Hou, Phys. Rev. B **62**, 10383 (2000).
[48] O. Robach, G. Renaud, and A. Barbier, Phys. Rev. B **60**, 5858 (1999).
[49] S. Mogck, B. J. Kooi, J. Th. M. De Hosson, and M. W. Finnis, Phys. Rev. B **70**, 245427 (2004).
[50] D. M. Duffy, J. H. Harding, and A. M. Stoneham, Philos. Mag. A **67**, 865 (1993).
[51] W. Vervisch, C. Mottet, and J. Goniakowski, Phys. Rev. B **65**, 245411 (2002).
[52] A. M. Ferrari and G. Pacchioni, J. Phys. Chem. **100**, 9032 (1996).
[53] L. Giordano, J. Goniakowski, and G. Pacchioni, Phys. Rev. B **64**, 075417 (2001).
[54] A. D. Vitto, G. Pacchioni, F. Delbecq, and P. Sautet, J. Phys. Chem. B **109**, 8040 (2005).